Nonsequential Double Ionization at the Single-Optical-Cycle Limit

X. Liu,[1] H. Rottke,[1] E. Eremina,[1] W. Sandner,[1] E. Goulielmakis,[2] K. O. Keeffe,[2] M. Lezius,[2] F. Krausz,[2,3] F. Lindner,[3] M. G. Schätzel,[3] G. G. Paulus,[4,5] and H. Walther[3,4]

[1]*Max-Born-Institut, Max-Born-Strasse 2a, D-12489 Berlin, Germany*
[2]*Institut für Photonik, Technische Universität Wien, Gusshausstrasse 27, A-1040 Wien, Austria*
[3]*Max-Planck-Institut für Quantenoptik, Hans-Kopfermann-Strasse 1, D-85748 Garching, Germany*
[4]*Ludwig-Maximilians-Universität München, Am Coulombwall 1, D-85748 Garching, Germany*
[5]*Department of Physics, Texas A&M University, College Station, Texas 77843-4242, USA*
(Received 15 June 2004; published 20 December 2004)

We report differential measurements of Ar^{++} ion momentum distributions from nonsequential double ionization in phase-stabilized few-cycle laser pulses. The distributions depend strongly on the carrier-envelope (CE) phase. Via control over the CE phase one is able to direct the nonsequential double-ionization dynamics. Data analysis through a classical model calculation reveals that the influence of the optical phase enters via (i) the cycle dependent electric field ionization rate, (ii) the electron recollision time, and (iii) the accessible phase space for inelastic collisions. Our model indicates that the combination of these effects allows a look into single cycle dynamics already for few-cycle pulses.

PACS numbers: 33.80.Rv, 33.80.Wz

Recent advances in femtosecond laser technology have opened the door to unprecedented insight into intense laser-matter interaction (up to 100 GW) on the time scale of a few optical cycles [1]. For such few-cycle pulses, the electric field $E(t) = E_0(t)\cos(\omega t + \varphi)$ depends strongly on the phase of the carrier wave (having frequency $\omega/2\pi$) with respect to the pulse envelope $E_0(t)$, the so-called carrier-envelope (CE) phase φ [2]. Since the pioneering work of [3] feedback control of this CE phase has been established [4] and a direct measurement of φ was demonstrated recently [5,6]. Today, the spatiotemporal variation of electromagnetic fields consisting of very few cycles is not only precisely known, but it can be shaped with attosecond precision via control over φ. Because of the exponential dependence of atomic tunnel ionization on the instantaneous electric field strength, control over φ has opened the opportunity to define the moment of ionization with a precision of several hundred attoseconds [7,8]. The trajectory of an electron born within this narrow time window remains subject to the laser field, which can, in principle, be tailored at will. This allows for control over various rescattering processes of the field liberated electron on the parent ion. Indeed, it has been found that for processes such as high harmonic generation (HHG) [5] and high-order above threshold ionization (ATI) [6] the experimentally observed outcomes are strongly dependent on φ. A third rescattering mechanism of paticular interest is present in nonsequential double ionization (NSDI) [9,10]. All the processes introduced here occur when a field accelerated electron returns and hits the parent ion it left before. The collision mechanisms can be classified as *recombination* (HHG), *elastic* (ATI), or *inelastic* (NSDI). The NSDI inelastic case causes dislodging of a second electron from the ion core and thus represents an excellent example for a heavily perturbed three-body Coulomb sys-

tem. Similar to HHG and ATI, a significant sensitivity on φ has already been predicted for the NSDI final state electron-electron momentum correlation [11]. This indicates the possibility to steer double ionization efficiently using φ. In this Letter we present the first experimental evidence that control over φ is indeed a suitable means to direct nonsequential double-ionization dynamics. Our data demonstrate a strong CE phase sensitivity of the differential momentum distribution of Ar^{2+} ions along the laser beam polarization axis. Moreover, our model calculation indicates that we are able to look into single cycle dynamics of NSDI even though the light pulses still consist of several cycles.

The experimental technique is based on cold target recoil ion momentum spectroscopy (COLTRIMS) [12]. Details of our experimental setup can be found in [13,14]. Briefly, a low-density (10^8 atoms/cm^3) supersonic argon atomic beam is intersected by a laser beam at its focal spot. A weak electric field (1–7 V cm^{-1}) extracts the ions created in the focus. Particles are recorded by a microchannel plate detector, and their initial momenta are determined from the measured time of flight and the position where they hit the detector. The solid angle of ion detection is 4π. Laser pulses are obtained from a commercial femtosecond oscillator and amplifier (Femtolasers GmbH) followed by a hollow fiber pulse compressor. 500 μJ pulse energy and 5 fs pulse width are produced at a center wavelength of 760 nm. The CE phase is stabilized using a three-stage servo loop. The first and second stages stabilize the phase of the oscillator and amplifier, respectively [5]. Both employ the self-referencing scheme known from optical frequency metrology [3]. Long-term phase stability (the measurements presented below required hours of data acquisition) is accomplished with the stereo-ATI method [6,15] by recording spectra of pho-

toelectrons emitted in opposite directions. These exhibit characteristic phase effects. Besides its use as a phase meter, the stereo-ATI helps in monitoring the laser performance. The experimental setup is sketched in Fig. 1. A small fraction (5%) of the laser radiation is rerouted to the stereo-ATI apparatus by use of a beam splitter. Precise adjustment of the amount of glass (W2) in the beam path corrects for the difference in optical path lengths to the stereo-ATI and to the COLTRIMS apparatus. This ensures short pulses in both experiments simultaneously. Control of W2, however, does not imply identical values of φ; in fact, the offset $\Delta\varphi = \varphi_{\text{ATI}} - \varphi_{\text{COLTRIMS}}$ as well as $\varphi_{\text{COLTRIMS}}$ itself is unknown during the experiment. However, what matters is that $\Delta\varphi$ is constant. In order to actively control the CE phase, the pair of glass wedges (W1) in the common beam path is equipped with a stepper motor and automatically controlled by the ATI phase meter. Hence, during the whole measurement the CE phase φ_{ATI} is measured and kept at a fixed value. In order to scan different values of $\varphi_{\text{COLTRIMS}}$, the amount of glass of W2 and therefore $\Delta\varphi$ is changed by known amounts. An addition of 26 μm of fused silica into the beam path changes φ by π.

Figure 2 shows Ar^{++} ion momentum ($P_{\parallel}$) distributions along the laser polarization direction for different CE phases measured at a fixed laser pulse width (≈ 5 fs) and intensity (≈ 350 TW/cm^2). The ion momentum resolution is 0.1 a.u. The spectra reflect the distributions of the corresponding sum-momentum component of the two photoelectrons [16]. A prominent asymmetric pattern is visible which changes with the CE phase. A nearly symmetric shape is found only at one setting of the phase ($\varphi = \varphi_0$). Switching off the phase stabilization of the laser gives rise to a symmetric ion momentum distribution [Fig. 2(f)]. It closely resembles "long" pulse spectra at light intensities where double ionization of Ar proceeds predominantly

nonsequential [13,16]. This, the observed strong phase sensitivity of the spectra, and our model calculation (see below) clearly indicate that nonsequential double ionization of Ar also prevails in the few optical cycle regime. Moreover, sequential double ionization with both electrons leaving the atom uncorrelated should show a similar phase dependence as single ionization, where integrated phase effects have been found to be of the order of only 10% [6]. This is much less than we find here for double ionization. The interesting points to be noted in Fig. 2 are as follows: (i) The fixed phase symmetric distribution ($\varphi = \varphi_0$) is slightly narrower than the distribution measured with the free-running phase at the same light intensity. (ii) The minimum in the Ar^{++} yield at $P_{\parallel} = 0$ is more pronounced in the fixed phase spectrum. (iii) A phase change of π transforms the momentum distribution into its mirror image with respect to reflection at $P_{\parallel} = 0$ [compare Figs. 2(a)–2(d) and 2(b)–2(e)].

In order to understand how the CE phase steers the ion momentum distribution and to determine φ_0, a classical model based on the light induced recollison mechanism of NSDI is applied to simulate the experimental results. This simple model has already been used successfully to analyze NSDI of molecules ionized by long laser pulses [14]. It is in remarkably good agreement with a more refined quantum mechanical calculation [17]. The idea behind our model is that NSDI is caused by an (e, $2e$) process induced by recollision of an electron on the singly charged ion core after it has been accelerated by the electric field of the light pulse. The recolliding electron is initially set free by field ionization at a time t_0 and collides with the ion core at a later time t_1. In turn, the probability for NSDI depends
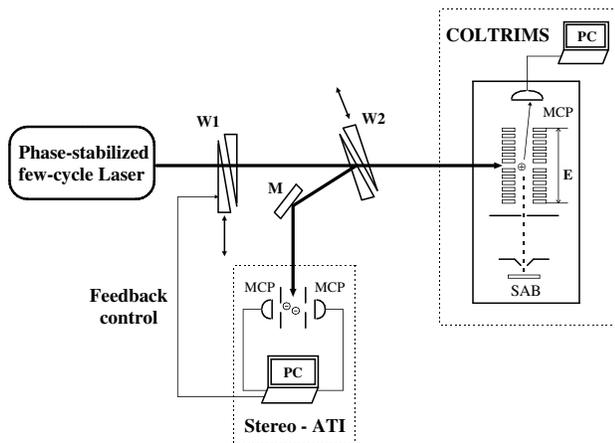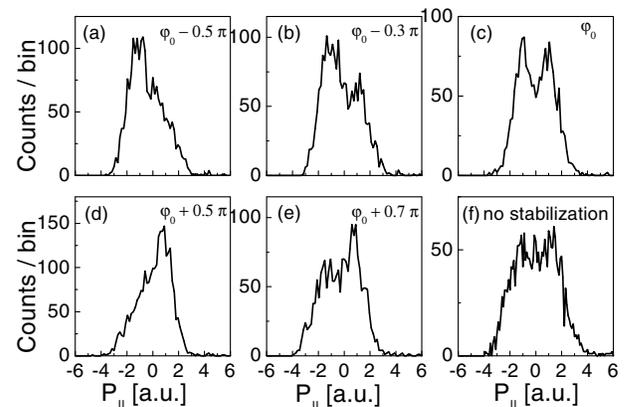

FIG. 1. Schematic view of the experimental setup. W1, W2: two pairs of glass wedges; MCP: position sensitive microchannel plate detector; M: mirror; E: extraction electric field; SAB: supersonic atomic beam.

FIG. 2. Experimental momentum distribution of Ar^{2+} ions from NSDI of Ar at different CE phases φ. The laser pulse parameters are ≈ 5 fs pulse width and ≈ 350 TW/cm^2 peak light intensity. The distributions are integrated over the Cartesian momentum components perpendicular to the light beam polarization axis. φ_0, shown on the panels, is determined from comparison with a theoretical model to be 0.2π. The spectrum in panel (f) was taken with the phase unstabilized at otherwise unchanged experimental parameters.

critically on the initial electric field ionization rate and on the kinetic energy $E_{kin}(t_1)$ of the electron at the time of recollision. Both the rate and $E_{kin}(t_1)$ depend sensitively on t_0. In our model NSDI is possible only at return energies which exceed the ionization potential of the singly charged ion.

For laser pulses with many cycles, field ionization at t_0 of an electron which recollides at $t_1 > t_0$ can happen at many oscillation maxima of $E(t) = E_0(t)\cos(\omega t + \varphi)$ ($\omega t + \varphi = n\pi$ with n an integer). At subsequent half-cycles n the electric field essentially only changes sign. This gives rise to a symmetric momentum distribution for the doubly charged ions with respect to reflection at $P_\| = 0$. In contrast, in a few-cycle pulse the amplitude of the electric field envelope changes significantly for successive half-cycles depending on the set CE phase φ. This is exemplified in the three upper panels of Fig. 3. Accordingly, the probability that an electron enters the continuum at some given time t_0 becomes sensitive to φ. This and the change in $E_0(t)$ between t_0 and t_1 breaks the symmetry for electron trajectories (see also [6]). In addition, the recollision time t_1 and the kinetic energy $E_{kin}(t_1)$ of the electron colliding with the ion core are depending on φ and will further amplify the left-right asymmetry. The classically accessible phase space for impact ionization by the returning electron is given by $E_{kin}(t_1) \geq I_p^+$, where I_p^+ is the ionization potential of the singly charged ion. Whether this threshold is reached depends significantly on successive half-cycles, as can be seen in the lower panel in Fig. 3. At each t_0 the light gray dotted line gives the maximum accessible momentum $p_{e,\|}$ one electron can aquire after impact ionization, and the black line the minimum momentum. Within every half-cycle the two lines thus characterize the outermost boundary of the classically accessible final phase space for the momentum component $P_\| = 2p_{e,\|}$ of Ar^{++} [19]. A missing border line in a half-cycle means that for electrons which are field ionized in this cycle $E_{kin}(t_1) < I_p^+$ upon recollision. The final momentum distribution of the doubly charged ion is determined by the interplay between three factors: the tunnel ionization rate as a function of t_0, the return time t_1, and $E_{kin}(t_1)$. Numerical results for the Ar^{++} momentum distribution are shown in Fig. 4. They are based on the classical model outlined above with an electron-electron contact interaction for the collision which is assumed to happen at the position of the ion core [17]. A gradual change of asymmetry appears with the center of gravity of the distribution shifting from negative to positive ion momentum with an increasing CE phase. A true symmetric distribution is not observed at any CE phase. Only near $\varphi = 0.2\pi$ (and 1.2π) a double hump structure with maxima of nearly equal strengths appears. However, the maxima do not appear at symmetric positions with respect to $P_\| = 0$, and the humps differ in width. We used the simulation to assign an absolute value of 0.2π to φ_0 (see Fig. 2). The accuracy of this assignment is about $\pm 0.1\pi$. Figure 2(f) demonstrates how sensitive the ion momentum distribution reacts to the width of the laser pulse. For an eight-cycle pulse the CE phase loses any influence on the momentum distribution, even at $\varphi = 0.7\pi$, a value where shorter pulses show the most pronounced asymmetry.

The simulation for $\varphi = -0.3\pi, 0.7\pi$ (Figs. 3 and 4) indicates that the major reason for the experimentally observed strong asymmetric ion momentum distributions is the birth of recolliding electrons within only one optical half-cycle ($t_0/T \approx -0.3\pi$ for both $\varphi = -0.3\pi$ and $\varphi = 0.7\pi$). A "beam" of scattering electrons hits the parent ion mainly from one side. Effective hits from the other side are
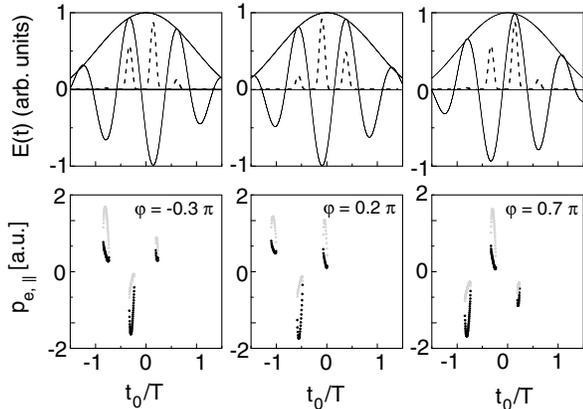

FIG. 3. Upper panel: electric field $E(t)$ (solid line) and the quasistatic field ionization rate [18] (dashed line) for a four-cycle laser pulse (760 nm center wavelength, 3.5×10^{14} W/cm^2 peak intensity). Lower panel: classically accessible final phase space upon recollision ($p_{1\|} = p_{2\|} = p_{e,\|}$) for electrons liberated at tunneling time t_0 (in units of the optical period $T = 2.6$ fs). φ denotes the corresponding CE phase.
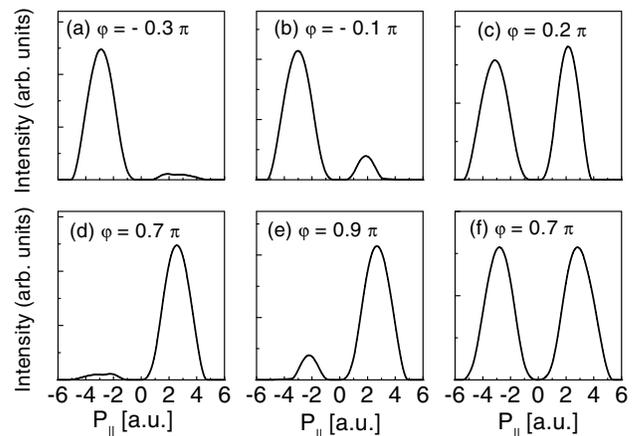

FIG. 4. Numerical simulation of the ion momentum distribution induced by few-cycle pulses at different CE phases. A four-cycle laser pulse is used in the calculation for (a)–(e) and an eight-cycle pulse in (f). The other parameters are the same as in Fig. 3.

suppressed by the combination of a small electric field ionization rate, and, in addition, lack of accessible phase space for the inelastic collision. Figure 3 ($\varphi = -0.3\pi$, $\varphi = 0.7\pi$) reveals that the inelastically scattering electrons which give rise to the predominating maxima in the corresponding ion momentum distributions in Fig. 4 are even not released during the half-cycle with the highest electric field strength. Regarding the "symmetric" case ($\varphi = 0.2\pi$) it is observed that two consecutive half-cycles contribute effectively to NSDI. The deviation from full symmetry of the double peak structure in Fig. 4(c) (widths and position of the two maxima) has the following origin: a significantly different accessible phase space and different field ionization rates in the two relevant half-cycles (see Fig. 3).

Overall we find the agreement between this simple model and our experimental results encouraging, even if a closer comparison yields some discrepancies. (i) The calculated yield of Ar^{++} ions with momentum $P_\parallel \approx 0$ is always close to zero, whereas the yield found in the experiment is significantly higher. Moreover, (ii) at $\varphi = -0.3\pi$ and at $\varphi = 0.7\pi$ nearly all ions are found with either $P_\parallel > 0$ or $P_\parallel < 0$ in the calculation. The experiment shows distributions with a clear "hanging shoulder" at these phases but a significant amount of ions is always found having an opposite momentum. In this respect it is important to note that a second significant NSDI channel exists for Ar. It is assumed to be the impact excitation of Ar^+ into bound excited states with subsequent electric field ionization of the excited electron [20]. This process allows the formation of photoelectron pairs with similar momenta emitted in opposing directions, giving rise to Ar^{++} ions with $P_\parallel \approx 0$. In our model this channel has not been incorporated. To learn more about the influence of this ionization channel it will be necessary to determine the final state electron momentum correlation [20]. (iii) The separation of the maxima in the experiment is smaller than that in the calculated spectra. However, the three-body contact interaction used here to describe the inelastic collision is known to result in a momentum separation usually larger than observed experimentally [21].

In conclusion, our experimental study shows that the ion momentum distribution following NSDI in few-cycle laser pulses reacts very sensitively to the CE phase φ. Consequently, via control over φ one is able to direct nonsequential double-ionization dynamics. The analysis of the experimental data through a classical model calculation reveals that the influence of the optical phase enters via (i) the cycle dependent electric field ionization rate, (ii) the electron recollision time, and (iii) the accessible phase space for inelastic collisions. It also shows that the combination of these effects allows a look into single cycle dynamics already if few-cycle pulses are used, since, de-

pending on the phase, only one or at most two optical half-cycles effectively contribute to NSDI. Being able to steer NSDI by control over the recolliding electrons via the CE phase goes well beyond NSDI itself. As proposed recently [7], recolliding electrons may be used as an effective probe for the attosecond time domain, comparable to the presently used attosecond extreme ultraviolet pulses [8]. Our work now demonstrates that it is possible to control electrons coherently in space and in time via control over the CE phase.

[1] M. Nisoli *et al.*, Opt. Lett. **22**, 522 (1997); G. Steinmeyer *et al.*, Science **286**, 1507 (1999).
[2] T. Brabec and F. Krausz, Rev. Mod. Phys. **72**, 545 (2000).
[3] J. Reichert, R. Holzwarth, Th. Udem, and T. W. Hänsch, Opt. Commun. **172**, 59 (1999); H. R. Telle *et al.*, Appl. Phys. B **69**, 327 (1999).
[4] D. J. Jones *et al.*, Science **288**, 635 (2000); A. Apolonski *et al.*, Phys. Rev. Lett. **85**, 740 (2000).
[5] A. Baltuška *et al.*, Nature (London) **421**, 611 (2003).
[6] G. G. Paulus *et al.*, Phys. Rev. Lett. **91**, 253004 (2003).
[7] H. Niikura *et al.*, Nature (London) **417**, 917 (2002).
[8] R. Kienberger *et al.*, Nature (London) **427**, 817 (2004)
[9] P. B. Corkum, Phys. Rev. Lett. **71**, 1994 (1993).
[10] R. Dörner *et al.*, Adv. At. Mol. Opt. Phys. **48**, 1 (2002).
[11] X. Liu and C. Figueira de Morisson Faria, Phys. Rev. Lett. **92**, 133006 (2004).
[12] J. Ullrich, R. Moshammer, A. Dorn, R. Dörner, L. Ph. Schmidt, and H. Schmidt-Böcking, Rep. Prog. Phys. **66**, 1463 (2003).
[13] E. Eremina, *et al.*, J. Phys. B **36**, 3269 (2003).
[14] E. Eremina *et al.*, Phys. Rev. Lett. **92**, 173001 (2004).
[15] G. G. Paulus *et al.*, Nature (London) **414**, 182 (2001).
[16] Th. Weber *et al.*, Phys. Rev. Lett. **84**, 443 (2000); R. Moshammer *et al.*, Phys. Rev. Lett. **84**, 447 (2000); Th. Weber *et al.*, J. Phys. B **33**, L127 (2000).
[17] C. Figueira de Morisson Faria, X. Liu, W. Becker, and H. Schomerus, Phys. Rev. A **69**, 021402(R) (2004).
[18] M. V. Ammosov, N. B. Delone, and V. P. Krainov, Zh. Eksp. Teor. Fiz. **91**, 2008 (1986) [Sov. Phys. JETP **64**, 1191 (1986)].
[19] C. Figueira de Morisson Faria and W. Becker, Laser Phys. **13**, 1196 (2003).
[20] B. Feuerstein *et al.*, Phys. Rev. Lett. **87**, 043003 (2001).
[21] R. Kopold, W. Becker, H. Rottke, and W. Sandner, Phys. Rev. Lett. **85**, 3781 (2000).